Slowed conduction and ventricular tachycardia after targeted disruption of the cardiac sodium channel gene *Scn5a*

G. Alex Papadatos*†, Polly M. R. Wallerstein*†, Catherine E. G. Head*‡, Rosemary Ratcliff*‡, Peter A. Brady*, Klaus Benndorf§, Richard C. Saumarez*¶, Ann E. O. Trezise‖, Christopher L.-H. Huang‡, Jamie I. Vandenberg*, William H. Colledge‡, and Andrew A. Grace*¶**

*Section of Cardiovascular Biology, Department of Biochemistry, University of Cambridge, Tennis Court Road, Cambridge CB2 1QW, United Kingdom; ‡Department of Physiology, University of Cambridge, Downing Street, Cambridge CB2 3EG, United Kingdom; ¶Department of Medicine, University of Cambridge, Addenbrooke's Hospital, Cambridge CB2 2QQ, United Kingdom; §Friedrich-Schiller-Universität Jena, Institut für Physiologie, Abteilung Herz-Kreislauf-Physiologie, 07740 Jena, Germany; and ‖Department of Anatomy and Developmental Biology, University of Queensland, St. Lucia Qld 4072, Australia

Communicated by Andrew Huxley, University of Cambridge, Cambridge, United Kingdom, March 1, 2002 (received for review September 21, 2001)

Voltage-gated sodium channels drive the initial depolarization phase of the cardiac action potential and therefore critically determine conduction of excitation through the heart. In patients, deletions or loss-of-function mutations of the cardiac sodium channel gene, *SCN5A*, have been associated with a wide range of arrhythmias including bradycardia (heart rate slowing), atrioventricular conduction delay, and ventricular fibrillation. The pathophysiological basis of these clinical conditions is unresolved. Here we show that disruption of the mouse cardiac sodium channel gene, *Scn5a*, causes intrauterine lethality in homozygotes with severe defects in ventricular morphogenesis whereas heterozygotes show normal survival. Whole-cell patch clamp analyses of isolated ventricular myocytes from adult *Scn5a*$^{+/-}$ mice demonstrate a ≈50% reduction in sodium conductance. *Scn5a*$^{+/-}$ hearts have several defects including impaired atrioventricular conduction, delayed intramyocardial conduction, increased ventricular refractoriness, and ventricular tachycardia with characteristics of reentrant excitation. These findings reconcile reduced activity of the cardiac sodium channel leading to slowed conduction with several apparently diverse clinical phenotypes, providing a model for the detailed analysis of the pathophysiology of arrhythmias.

Cardiac arrhythmias, manifest clinically by symptoms of extra, slow, or rapid heart beats, form one of the most common groups of diseases (1). The detailed understanding of the pathophysiology of these conditions now seems possible (2), having been advanced by the identification of ion channel mutations in patients with these conditions (3–5). What has become clear is that the functional consequences of such mutations can be complex, resolved only by combining appropriate clinical, experimental, and theoretical approaches (2). Accordingly, the consequences of gain-of-function mutations in the cardiac sodium channel gene, *SCN5A*, in patients with long-QT syndrome (LQT3) (6, 7), have been investigated by studies of clinical genotype–phenotype relationships (3–5, 8) and their cellular electrophysiology (9, 10) by using computer models (11, 12) and the construction of a transgenic mouse (13). The results of these various investigations have allowed a clearer picture to emerge of the pathophysiology of LQT3 (7).

In addition to the descriptions of long-QT syndrome-associated mutations, loss-of-function mutations in *SCN5A* (14, 15) have been described in patients with phenotypic characteristics of bradycardia (16, 17), atrioventricular block (16, 18), and ventricular fibrillation (18–22). These observations suggest a central role for the sodium channel in the maintenance of the normal heart beat (23–25). The mechanism of arrhythmias in these conditions, however, remains unresolved, although fibrillation could result from delayed conduction, unidirectional block, and reentrant excitation (3, 4). We have used homologous recombination in embryonic stem cells to establish mice with a null mutation in the sodium channel gene, *Scn5a*, to provide an experimental system to examine both the pathophysiology of these clinical conditions and to assess the physiological contribution of sodium channels to cardiac impulse initiation and propagation. The phenotypes of wild-type and *Scn5a*$^{+/-}$ hearts were compared *in vivo*, using surface electrocardiogram (ECG) recordings, and also *ex vivo*, using epicardial recordings in isolated Langendorff-perfused preparations.

Materials and Methods

Generation of *Scn5a*-Deficient Mice. PCR primers corresponding to the known human and rat *SCN5A* exon 2 sequences (15) were used to amplify a 200-bp probe from wild-type 129Sv/Ev DNA. The labeled probe was used to screen a P1 artificial chromosome-based mouse genomic library (Incyte Genomics, St. Louis). One P1 clone was isolated and a targeting vector made by subcloning a 6.4-kb *Bam*HI-*Eco*RV genomic fragment. Exon 2 was replaced with a splice acceptor (SA)-*Gfp*-PGK-neomycin cassette (Fig. 1*A*) (26) by using established techniques (27). *Gfp* was inserted as a reporter gene for *Scn5a* expression. The 5′ and 3′ arms of the targeting vector were 656 and 3,350 bp, respectively. A thymidine kinase cassette was cloned into the 3′ end of the vector as negative selection against random integration. The vector was linearized at a unique *Bam*HI site on the 5′ end of homology. After electroporation of embryonic stem cells, targeted clones were identified by PCR at the 5′ end and confirmed by Southern blotting of the 3′ end with an external probe (Fig. 1*B*). Correctly targeted clones were injected into C57BL/6J blastocysts to generate male chimeras that were crossed with C57BL/6J females to give F1 heterozygous offspring (*Scn5a*$^{+/-}$). These were identified by PCR screening (Fig. 1*C*) with three primers (Scnint1F, GTTCTTGTGTTCCTGTCCGGC; Scnex2R, GGGTGGGTTGCCATAGAGATC; ScnVect1R, GGAAAACCCTGGACTACTGCG). Mice were inbred onto a 129/Sv genetic background. Experimental studies were performed on these inbred mice when they were 8–10 weeks of age unless stated otherwise. All animal experimentation was carried out in accordance with governmental and institutional guidelines.

Patch Clamp Electrophysiology. Enzymatically dissociated adult ventricular myocytes were prepared from wild-type and *Scn5a*$^{+/-}$ mice as described (28). Borosilicate glass patch pipettes were used for patch clamp electrophysiological measurements. Pipettes had resistances of 0.8–2.0 MΩ and were filled with internal solution

Abbreviations: S2, every ninth stimulus; S1, all other stimuli; E*n*, embryonic day *n*; ECG, electrocardiogram.

See commentary on page 5755.

†G.A.P. and P.M.R.W. contributed equally to this work.

**To whom reprint requests should be addressed. E-mail: ag@mole.bio.cam.ac.uk.

The publication costs of this article were defrayed in part by page charge payment. This article must therefore be hereby marked "*advertisement*" in accordance with 18 U.S.C. §1734 solely to indicate this fact.

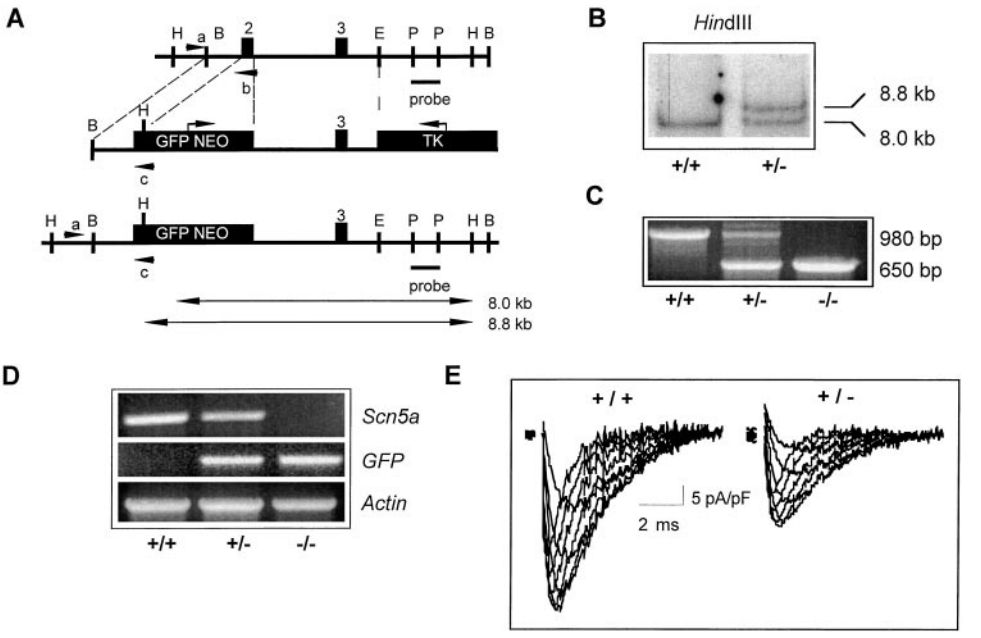

Fig. 1. Disruption of *Scn5a* locus. (*A*) Structure of wild-type *Scn5a* locus, targeting vector, and targeted locus. Insertion of neo cassette replaced the first coding exon. Restriction sites (B, *Bam*HI; H, *Hin*dIII; P, *Pst*I; E, *Eco*RV) and the probe used for detection of the homologous recombination event by Southern analysis are shown. Expected fragment sizes of wild-type (8.0 kb) and mutant alleles (8.8 kb) after *Hin*dIII digestion are indicated. PCR primers used for screening of embryonic stem (ES) cells and genotyping of mouse tail DNA are shown (*a–c*). TK, thymidine kinase; GFP, green fluorescent protein. (*B*) Southern blot of *Hin*dIII-digested ES cell DNA. (*C*) PCR genotyping of E10.5 embryos identifying wild type, *Scn5a*$^{+/-}$, and *Scn5a*$^{-/-}$. (*D*) Reverse transcription–PCR analysis of *Scn5a*, *GFP*, and *Actin* transcripts in *Scn5a*$^{-/-}$, *Scn5a*$^{+/-}$, and wild-type embryos. *Scn5a* deletion is confirmed in *Scn5a*$^{-/-}$ mutants with transcription of *GFP* and *Actin* as controls. (*E*) Typical examples of currents recorded from wild-type and heterozygous myocytes during depolarization steps from −100 mV to voltages between −50 to −15 mV in 5-mV increments (see Table 1). The peak current densities in wild-type myocytes were typically larger than those in *Scn5a*$^{+/-}$ myocytes (see text for details).

containing 2 mM NaCl, 140 mM CsCl, 10 mM Hepes, and 10 mM EGTA (pH adjusted to 7.4 with CsOH). The perfusion solution contained 2 mM NaCl, 1 mM $MgCl_2$, 0.1 mM $CaCl_2$, 10 mM glucose, 140 mM CsCl, and 10 mM Hepes (pH 7.4). Nicardipine (2 μM) was added to solutions to block I_{Ca}. Experiments were consistently performed at room temperature (≈22°C), which provided comparisons of maximum current and an indication of any kinetic differences between currents in wild-type and *Scn5a*$^{+/-}$ cells. Current recordings were made by using an Axopatch 200B amplifier (Axon Instruments, Foster City, CA). Capacitance current transients were electronically subtracted with series resistance compensation typically at 80%. Current signals were filtered at 10 kHz and sampled at 20 kHz. All current traces were leak-subtracted offline (28, 29). Leak was assumed to be linear with voltage and determined from the average of four pulses from −100 mV to −30 mV. Acquisition and analysis of data used PCLAMP6 software (Axon Instruments).

Electrocardiography. Mice were lightly anesthetized with i.p. ketamine (100 mg kg^{-1}) and xylazine (5 mg kg^{-1}). Three-lead ECGs

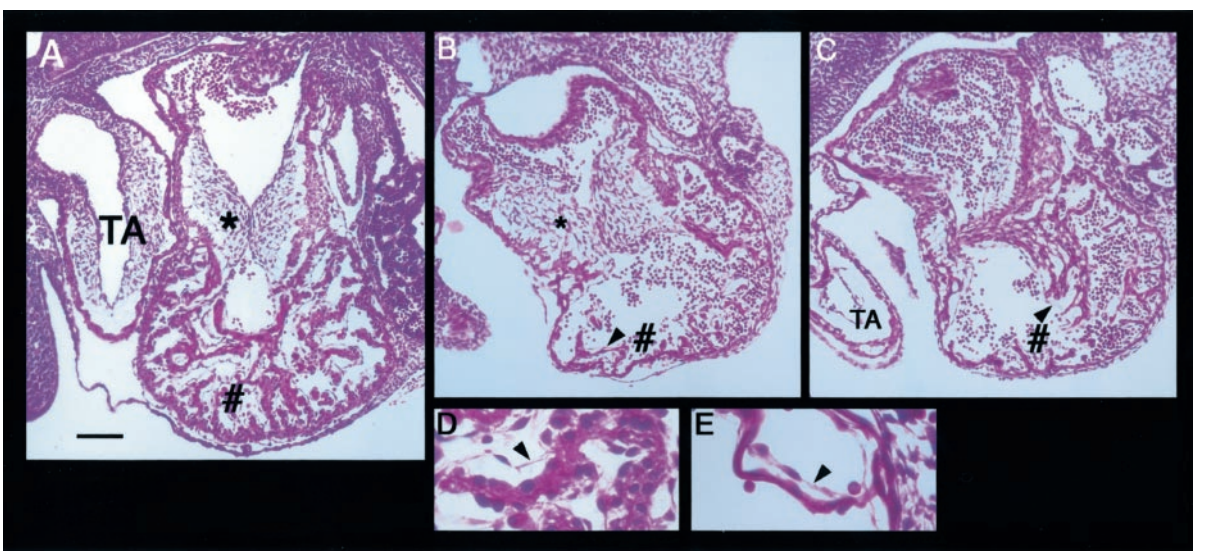

Fig. 2. Morphology of E10.5 wild-type and *Scn5a*$^{-/-}$ hearts. Nine *Scn5a*$^{-/-}$ embryos and four control embryos (wild type or *Scn5a*$^{+/-}$) were examined. (*A*) Representative sagittal paraffin section of a control E10.5 heart stained with hematoxylin and eosin. The myocardial wall of the common ventricular chamber shows extensive trabeculation (#) and the endocardial cushions of the atrioventricular canal (*) are well developed. Also, at this stage the truncus arteriosus (TA) shows the first signs of the formation of the aorticopulmonary spiral septum. (*B* and *C*) Representative sections of hearts from E10.5 *Scn5a*$^{-/-}$ embryos. Note the well developed endocardial cushions (*) and TA but little trabeculation of the ventricular wall (#). (*D* and *E*) High-magnification views of the cardiomyocytes and endothelial cells from control (*D*) and *Scn5a*$^{-/-}$ (*E*) embryos. Arrowheads (in *B–E*) indicate the endothelial cell layer surrounding the trabeculated myocardium and lining the ventricular chamber. [Bar = 100 μm (in *A–C*) and 25 μm (in *D* and *E*).]

Table 1. Parameters of whole-cell sodium current

Myocyte	Current density (pA/pF)	Steady-state activation		Steady-state inactivation	
		$V_{1/2}$, mV	k, mV	$V_{1/2}$, mV	k, mV
Wild type	37 ± 9 (n = 6)	−41.8 ± 3.0	6.0 ± 0.7 (n = 4)	−75.2 ± 4.9	8.1 ± 0.2 (n = 4)
Scn5a$^{+/-}$	21 ± 5 (n = 5)*	−39.2 ± 4.1	6.2 ± 1.0 (n = 4)	−74.4 ± 2.7	8.2 ± 0.2 (n = 3)

Steady-state activation and inactivation of whole-cell sodium channel conductances were fitted with a Boltzmann equation: $g = g_{max}/\{1 + \exp[(V - V_{1/2})/k]\}$, where g is conductance, g_{max} is maximal value of conductance, $V_{1/2}$ is voltage of half-maximal activation/inactivation, and k is the slope factor. *, $P < 0.05$ comparing wild-type and Scn5a$^{+/-}$ ventricular myocytes. All other measurements not significantly different in the two groups.

were recorded with surface limb electrodes and a standard clinical device (Sanborn Visette, Waltham, MA). At least six estimations of each ECG interval in leads I and II were made for each mouse, and the means were calculated. The measured complexes were those where onset and termination were most clearly defined and complexes were not sampled from recordings containing baseline instabilities (e.g., see Fig. 3*A*). Standard criteria were used for interval measurements: P wave duration (representing intraatrial conduction) from the onset of the P wave to the point where the P wave returns to the isoelectric line; the PR interval (as a result of combined intraatrial and atrioventricular nodal conduction) from the P wave onset to the onset of the QRS complex (representing ventricular depolarization); the end of the QRS complex could not be measured accurately (30), and QRS duration is not reported. Finally, the QT interval (reflecting the combined time interval covering ventricular depolarization and repolarization) is measured from the onset of the QRS complex to the end of the T wave.

Perfused Heart Electrophysiology. Mouse hearts were Langendorff-perfused with Krebs–Henseleit solution (31) at a perfusion pressure of 60–90 mmHg corresponding to a flow rate of 2.1 ± 0.3 ml min^{-1} (mean ± SD, n = 8) at 37°C, and hearts paced at 10 Hz for 20–30 min until stable. In all hearts, pacing stimuli of 2-ms pulse duration and amplitude of 0.5–1.0 V, corresponding to twice-threshold in both wild-type and *Scn5a*$^{+/-}$ mice, were used. Signals were subject to band-pass filtering between 3 Hz and 1 kHz.

Perfused ventricular preparations. Atria were removed, and bipolar platinum electrodes of 1-mm interpole spacing were attached to the mid-right ventricular septum for pacing and the basal portion of the left ventricular epicardium for recording. Most studies were conducted with intervals between stimuli of 100 ms except that every ninth stimulus (designated as S2) followed the preceding stimulus at an interval that was reduced progressively by 1-ms steps, starting at 99 ms. All stimuli except S2s are designated as S1 and they follow the preceding stimulus at an interval of 100 ms (32). The sequence was continued with progressively decreasing S1-S2 stimulus intervals until the S2 stimulus failed to excite the myocardium at the ventricular effective refractory period.

Perfused whole heart preparation. To assess atrioventricular conduction the atria were not removed, and the stimulating electrodes were attached to the right atrium with recording from the left ventricle. Atrial pacing began with an interval between successive stimuli of 100 ms. This stimulus interval (S1-S1) was then reduced by 1 ms every 10–20 beats until this failed to excite the ventricle.

Statistics. All data are expressed as means ± SD. Statistical analysis of all processed data were performed with Microsoft EXCEL software; comparisons were made with Student's t test (a value of $P < 0.05$ being considered significant). The number of experiments (n) in all cases refers to the use of different preparations.

Results and Discussion

***Scn5a* Mutant Mice.** No *Scn5a*$^{-/-}$ mice resulted from the interbreeding of *Scn5a*$^{+/-}$ mice, suggesting embryonic lethality. In *Scn5a*$^{-/-}$ embryos (n = 17), some hearts were seen to show uncoordinated contractions up to embryonic day (E) 10.5, but no contraction was observed beyond E11.5 with autolysis of embryos supervening (n = 16). Lack of *Scn5a* expression in *Scn5a*$^{-/-}$ embryos was confirmed by reverse transcription (RT)-PCR (Fig. 1*D*). *GFP* (GFP, green fluorescent protein) expression was detected in *Scn5a*$^{+/-}$ and *Scn5a*$^{-/-}$ animals by RT-PCR (Fig. 1*D*) but was below the sensitivity of detection by microscopy. To investigate the cause of the

Table 2. ECGs and perfused heart electrophysiology

Parameter	Wild type (n)	Scn5a$^{+/-}$ (n)	Significance
ECGs*			
RR interval, ms	177 ± 38 (9)	193 ± 37 (9)	NS
P wave duration, ms	19 ± 3 (8)	24 ± 6 (9)	$P < 0.05$
PR interval, ms	41 ± 4 (9)	56 ± 6 (9)	$P < 0.001$
QT interval, ms	45 ± 5 (9)	49 ± 7 (9)	NS
Intact Langendorff-perfused hearts			
Cycle length, ms	123 ± 5 (9)¶	420 ± 47 (6)	$P < 0.001$
Atrioventricular nodal refractory period, ms†	42 ± 3 (4)	69 ± 4 (4)	$P < 0.001$
Perfused ventricular preparations			
Cycle length, ms	248 ± 23 (8)¶	No cardiac activity	
Stimulus-response latency, ms‡	9 ± 1 (9)	18 ± 1 (6)	$P < 0.001$
Complex duration, ms‡	32 ± 3 (9)	64 ± 2 (6)	$P < 0.001$
Ventricular effective refractory period, ms§	29 ± 1 (9)	56 ± 7 (6)	$P < 0.001$

¶, $P < 0.001$ comparing atria present and atria absent. All data are expressed as means ± SD. Statistical comparisons used Student's t test with $P < 0.05$ considered significant. n in all cases refers to the use of different preparations. NS, not significant. See *Materials and Methods* for details of ECG intervals.

†Point of failure of atrioventricular conduction during atrial pacing (see text and *Materials and Methods* for detail).

‡Stimulus-to-response latency and complex duration measured during constant pacing (S1-S1) at a cycle length of 100 ms.

§Ventricular effective refractory period obtained during decremental stimulation runs with initial stimulus interval (S1-S2) of 99 ms (see Fig. 4*D*). The ventricular effective refractory period is the longest S1-S2 that does not produce a propagated response.

embryonic lethality in the homozygous mutant mice, we sectioned embryos at E10.5. The *Scn5a*$^{-/-}$ embryos were smaller than their *Scn5a*$^{+/-}$ and wild-type littermates. Developmental defects were seen most strikingly in the common ventricular chamber of the heart (Fig. 2). Comparisons of Fig. 2 *A–E* reveal hearts of *Scn5a*$^{-/-}$ embryos to have reduced chamber size, reduced trabeculation of the ventricular wall, and a reduced number of thin, spindle-like cardiomyocytes compared with hearts from control animals. This ventricular defect in *Scn5a*$^{-/-}$ embryos is unlikely to reflect simply a generalized failure of cardiac development, because the endocardial cushions of the atrioventricular canal, the common atrial chamber, and the truncus arteriosus all appear normal. Also, the endothelial cells that cover the developing myocytes and line the ventricle are clearly present in both control and *Scn5a*$^{-/-}$ embryos (arrowheads in Fig. 2 *B–E*). The mechanisms whereby the loss of SCN5A leads to this gross defect in ventricular morphogenesis have not been examined but are likely to be a direct result of the loss of *Scn5a* and not secondary to circulatory failure. This contention is supported by the similar phenotype described in the *island beat* (*isl*) mutation in zebrafish that displays selective failure of ventricular development (33). Positional cloning has localized *isl* loss-of-function mutations to the pore-forming α1C subunit of the L-type calcium channel (33). The possibility that ion channels have an important influence on ventricular development is thereby further supported (33).

Scn5a$^{+/-}$ Mice Have Reduced Sodium Channel Density. *Scn5a*$^{+/-}$ mice developed normally with no difference in mortality compared with wild type. Hearts from adult (aged 8–10 weeks) *Scn5a*$^{+/-}$ and wild-type mice had identical weights (and heart/body weight ratio) and no obvious structural abnormalities. Fig. 1*E* displays typical currents from wild-type and *Scn5a*$^{+/-}$ ventricular myocytes. Peak current densities for *Scn5a*$^{+/-}$ myocytes (21 ± 5 pA/pF, $n = 5$) were reduced compared with wild type (37 ± 9 pA/pF, $n = 6$, $P < 0.01$), with the peak I_{Na} not significantly different from 50% of the peak wild-type value (pA/pt, picoampere/picofarad). Half-activation voltages ($V_{1/2}$) and slope factors (k) for steady-state activation and inactivation and rates of inactivation were statistically indistinguishable (Table 1). *Scn5a*$^{+/-}$ mice therefore have reduced sodium channel density with virtually identical channel-gating characteristics.

ECGs of Scn5a$^{+/-}$ Mice. ECGs indicated similar heart rates in lightly anesthetized wild-type and *Scn5a*$^{+/-}$ mice (Table 2), implying no apparent sodium current contribution to resting heart rate *in vivo* and consistent with observations in adult rabbit heart (34). ECG recordings from *Scn5a*$^{+/-}$ mice indicated slow conduction within the atria and atrioventricular conduction system evidenced by extreme prolongation of both the P wave and the PR interval (Fig. 3*B* and Table 2). A more pronounced conduction defect was observed in 2 of 9 *Scn5a*$^{+/-}$ mice with a failure of alternate atrial impulses to excite the ventricles (Fig. 3*C*), which was consistent with clinical features of type II second-degree atrioventricular block. There was also a rightward shift in the cardiac axis in three mice, suggesting defective intraventricular conduction (Fig. 3*C*). In contrast, the QT interval was unchanged in these *Scn5a*$^{+/-}$ mice, suggesting that noninactivating sodium channels (29) are unlikely to influence significantly the duration of ventricular repolarization.

Electrophysiology of Whole Isolated Scn5a$^{+/-}$ Hearts with Atria Intact. After aortic cannulation and Langendorff-perfusion, whole *Scn5a*$^{+/-}$ hearts showed marked rate slowing (cycle length, 420 ± 47 ms, $n = 6$) compared with wild type (123 ± 5 ms, $n = 9$, $P < 0.001$). This observation can be attributed to reduced excitability caused by a decreased number of sodium channels. This dramatic difference from the *in vivo* situation, where the heart rate is not significantly reduced in *Scn5a*$^{+/-}$ mice compared with wild type, is consistent with a significant autonomic contribution to the maintenance of impulse initiation and conduction in *Scn5a*$^{+/-}$ mice. The properties of the specialized conduction system of *Scn5a*$^{+/-}$ and wild-type mice were examined with incremental atrial pacing. Paced atrial beats blocked at stimulus intervals (S1-S1) in wild-type hearts (42 ± 3 ms, $n = 4$, Fig. 3*D*) comparable to previous measurements reported *in vivo* (35). In contrast, *Scn5a*$^{+/-}$ hearts showed significant impairment of impulse propagation with paced atrial beats being blocked at S1-S1 intervals of 69 ± 4 ms ($n = 4$, $P < 0.001$ compared with wild type, Fig. 3*E*). These findings are consistent with both increased atrial refractoriness and with limits on atrioventricular conduction. However, the findings of prolonged PR intervals and shifts in the dominant electrical axis on *in vivo* surface ECG recordings taken together with the *ex vivo* findings suggest significant atrioventricular conduction failure (Table 2). They are similar to clinical observations in patients with loss-of-function *SCN5A* mutations (16–18, 20) and may indicate that sodium channels are functionally more important to the mainte-

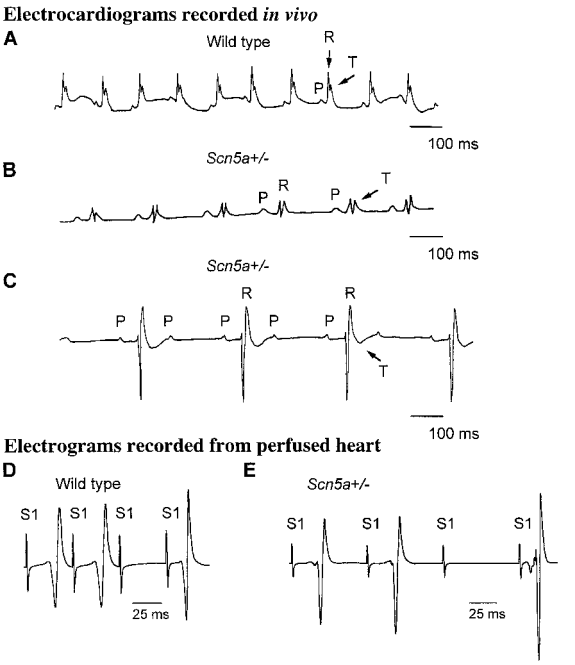

Fig. 3. ECGs and atrioventricular conduction in wild-type and *Scn5a*$^{+/-}$ mice. (*A*) Representative single-lead ECG strip (standard lead I) from wild-type mouse with P waves (P) caused by atrial depolarization, QRS complexes (R) caused by ventricular depolarization, and T waves (T) caused by ventricular repolarization. The cycle length is 120 ms with successful 1:1 conduction from the atria to the ventricles. P wave duration (18 ms) and PR interval (35 ms) are comparable to those reported for mouse (35). (*B*) Lead I of representative ECG taken from *Scn5a*$^{+/-}$ mouse showing 1:1 atrioventricular conduction and cycle length of 220 ms. There is increased P wave duration (26 ms) and prolonged PR interval (60 ms) when compared with wild type. (*C*) Rhythm strip (lead II) taken from *Scn5a*$^{+/-}$ mouse showing conduction of only every second atrial beat (P) to the ventricle (R), indicating *second-degree* atrioventricular block. Atrial cycle length is 170 ms, and ventricular cycle length is 340 ms. The PR interval is prolonged (60 ms) with a rightward shift in the QRS axis indicative of widespread atrioventricular conduction delay (outbred *Scn5a*$^{+/-}$ mouse) with associated T wave inversion. (*D*) Characteristics of atrioventricular nodal conduction in wild-type Langendorff-perfused heart during right atrial pacing and left ventricular epicardial recording. Far-field atrial pacing stimulation artifacts (S1) and resulting ventricular electrograms are shown. The stimulus interval of the paced beats (S1-S1) is progressively reduced with the third artifact shown delivered at a stimulus interval of 42 ms and not conducted to the ventricle (Wenckebach block), which is compatible with previous results obtained *in vivo*, e.g., controls in the description of the phenotype of *connexin40* mutant mice (35). (*E*) Representative recording from *Scn5a*$^{+/-}$ hearts obtained under identical conditions to *D*. In this example, atrioventricular conduction is significantly impaired with the third atrial paced beat (S1) delivered at a stimulus interval (S1-S1) of 70 ms not conducted to the ventricle (see Table 2).

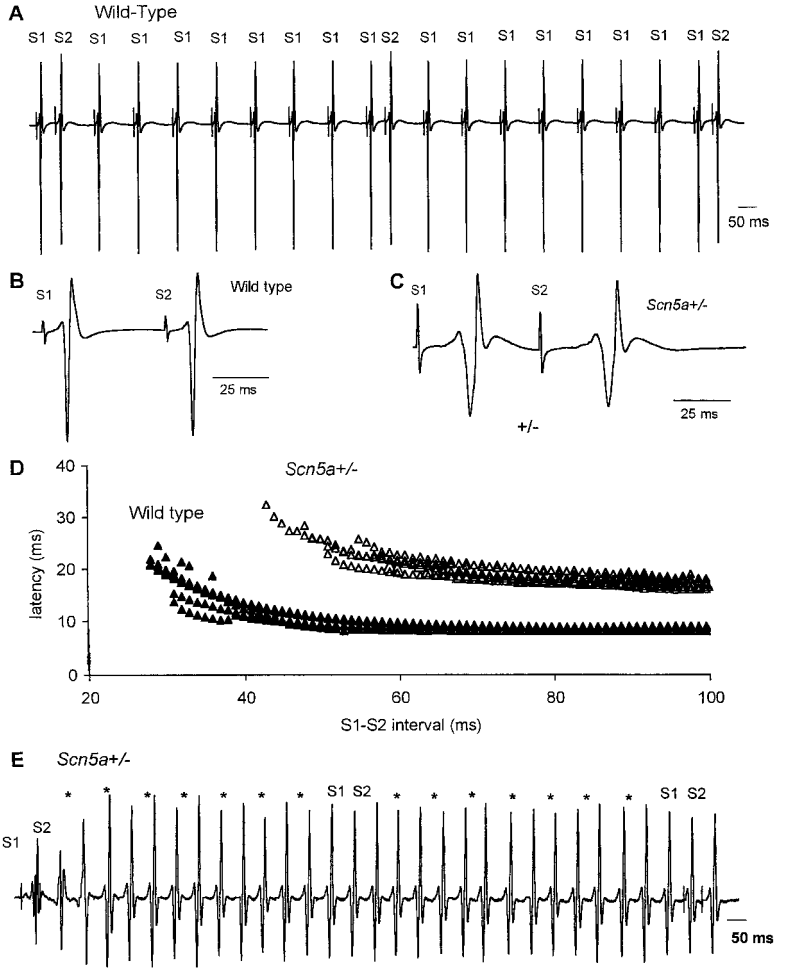

Fig. 4. Assessment of conduction properties and ventricular tachycardia in Langendorff-perfused mouse ventricular preparations. (*A*) Illustration of continuous electrical recordings from the base of the left ventricle in response to stimuli applied to the right ventricular septum. The interval between stimuli is 100 ms except that S2 follows the preceding S1 stimulus at an interval that is decreased progressively in 1-ms steps, starting at 99 ms. In this example, the three S1-S2 intervals shown are (left to right) 49, 48, and 47 ms. (*B*) Earlier section of trace shown in *A* on expanded time base (× 5.8). S1-S2 interval 55 ms. (*C*) Recording from *Scn5a*$^{+/-}$ ventricle, also with S1-S2 interval 55 ms. Latency and duration of electrogram are greater in *Scn5a*$^{+/-}$ than in wild type (24 and 56 ms, respectively, after S1 in *C*; 10 and 40 ms in *B*). After S2, latency is considerably increased (13 ms in *B* and 32 ms in *C*) whereas duration is only slightly increased. The number of components in the electrogram [termed fractionation (32, 42)] is not increased in the *Scn5a*$^{+/-}$ preparation. (*D*) Latency of electrogram in response to each S2 stimulus was measured in a record similar to *A* and is plotted here against the corresponding S1-S2 interval for 9 wild-type preparations (filled triangles) and for 6 *Scn5a*$^{+/-}$ preparations (open triangles). For all S1-S2 intervals, latency is much longer in *Scn5a*$^{+/-}$ than in wild type. The ventricular effective refractory period (value of S1-S2 interval as which response fails) is greater in *Scn5a*$^{+/-}$ (56 ± 7) than in wild type (29 ± 1, $P < 0.001$). (*E*) Representative electrical recording from *Scn5a*$^{+/-}$ ventricular preparation. S2 delivery at 49-ms stimulus interval (far left of trace) is followed by a delayed (latency, 52 ms) ventricular response that initiates ventricular tachycardia (asterisks represent points of S1 delivery with shock artifacts removed for clarity). The tachycardia is organized, and monomorphic of mean cycle length is 64 ms (the cycle length in individual traces varied in the range of 60–70 ms). There is no response to the delivery of S1 stimuli at 100-ms cycle length (asterisks). Delivery at an S1-S2 stimulus interval of 47 ms captures the ventricle (only ≈15 ms after the end of the previous ventricular depolarization) and terminates the tachycardia.

nance of normal atrioventricular conduction than previously considered (36, 37).

Electrophysiology of Isolated *Scn5a*$^{+/-}$ Ventricular Preparations. We anticipated that removal of supraventricular pacemaker cells would unmask further differences between the two mouse lines. In wild-type mice, complete atrial removal resulted in the anticipated junctional/ventricular rhythm, and contraction continued albeit significantly more slowly (cycle length, 248 ± 23 ms, $n = 8$, see Table 2). In contrast, without atria, *Scn5a*$^{+/-}$ ventricular preparations lost all spontaneous electrical activity. Moreover, intrinsic spontaneous activity failed to resume after pacing ceased in *Scn5a*$^{+/-}$ ventricular preparations whereas it returned almost immediately in wild-type preparations. Each of these observations is compatible with reduced cardiac excitability caused by a generalized decrease in the availability of I_{Na} for fast-membrane depolarization and a reduced safety margin for impulse initiation and conduction in *Scn5a*$^{+/-}$ mice, as would be predicted by the Luo–Rudy ventricular cell computer model (38). We next examined conduction and refractoriness during pacing in these ventricular preparations. The pacing protocols used an index pacing frequency of 10 Hz with a stimulus interval (S1-S1) of 100 ms. These values roughly correspond to the range of heart rates measured by telemetric recording methods in the free-ranging laboratory mouse (39–41). Fig. 4*A* illustrates how responses to S2 stimuli delivered at progressively shorter S1-S2 intervals after the preceding S1 pacing stimulus are used to detect changes in intraventricular conduction (32, 42). Conduction curves, which characterize myocardial conduction between the pacing and recording electrodes (Fig. 4*D*), were derived from individual electrograms obtained from wild-type (Fig. 4*B*) and *Scn5a*$^{+/-}$ mice (Fig. 4*C*). *Scn5a*$^{+/-}$ mice demonstrated slowed conduction with an increased delay between the pacing artifact and the appearance of the sensed electrogram when paced at a cycle length of 100 ms (18 ± 1 ms, $n = 6$; Fig. 4*D*, open triangles) compared with wild type (9 ± 1 ms, $n = 9$; Fig. 4*D*, filled triangles, $P < 0.001$; Table 2). This delay is unlikely to be the result of the setting up of the action potential as the ventricular electrogram duration is also increased in *Scn5a*$^{+/-}$ mice (64 ± 2 ms, $n = 6$) relative to ventricles from wild-type animals (32 ± 3 ms, $n = 9$, $P < 0.001$; Table 2). The introduction of S2 stimuli at S1-S2 intervals reduced in 1-ms decrements from 99 ms to ventricular refractoriness resulted in progressively increased latencies to the first component of the S2-initiated ventricular electrogram in both wild-type and *Scn5a*$^{+/-}$ ventricles (Fig. 4*D*). This response, with its corresponding increases in latency until propagation ceases (at the ventricular effective refractory period), is also characteristic of human ventricular myocardium examined *in vivo* (32, 42). Latency is approximately doubled in *Scn5a*$^{+/-}$ compared with wild-type ventricles at each S1-S2 stimulus interval (Fig. 4*D*). These observations confirm that sodium current magnitude critically influences impulse conduction (23, 24). Although many other factors may determine cardiac syncytial conduction (43), including the heterogeneous distributions of cardiac ion channels, such factors were not reflected in these experiments; ventricular preparations from *Scn5a*$^{+/-}$ mice showed no increase in the number of electrogram deflections (compare Fig. 4 *B* and *C*) (32, 42) that might suggest increases in the dispersion of conduction or repolarization (43) as reported in patients with primary ventricular fibrillation (42). The

absence of such evidence for dispersed conduction in the mouse may be species-related. It may require gradients of ion channel expression (44, 45) or the presence of mid-myocardial (M) cells so well described in other species (43, 46) but not thus far in mouse. Finally, *Scn5a*$^{+/-}$ preparations showed large increases in refractory periods (Fig. 4*D*, Table 2) such that the ventricle failed to respond to pacing (despite increases in the amplitude of the pacing stimulus to 4-fold threshold) and it was not possible to pace more rapidly than 14–16 Hz in *Scn5a*$^{+/-}$ ventricle compared with up to 20 Hz in wild type. Although action potentials were not measured in isolated ventricular preparations, similar QT intervals on surface ECGs suggest that action potential duration is unlikely to be significantly different in *Scn5a*$^{+/-}$ and wild-type mice. Increased refractoriness is therefore most likely the result of a reduced pool of sodium channels available to facilitate the recovery of excitability (24, 47, 48).

Ventricular Tachycardia in *Scn5a*$^{+/-}$ Ventricular Preparations. Ventricular tachycardia was consistently observed in 4 of 6 of the *Scn5a*$^{+/-}$ (Fig. 4*E*) but not in wild-type ventricular preparations ($n = 9$, Fig. 4*A*) during continuous pacing or after the delivery of S2 stimuli at shorter S1-S2 intervals. In the two *Scn5a*$^{+/-}$ preparations that did not develop tachycardia, the ventricular effective refractory period was markedly prolonged (both ≈65 ms), under which conditions the possibilities for reentrant excitation are likely to have been reduced (47). During programmed stimulation in the remaining ventricular preparations from *Scn5a*$^{+/-}$ mice, tachycardia was induced at stimulus intervals between 41 and 49 ms. These tachycardias were induced reproducibly in individual preparations and have the appearances of monomorphic ventricular tachycardia (see Fig. 4*E*). The cycle length of the tachycardia (≈64 ms) is compatible with the presence of a single axis of rotation with the rotation period similar to that reported in mouse heart (≈70 ms) (49). Tachycardia duration varied and although self-termination was occasionally observed after periods of up to several minutes in two preparations, sustained tachycardia was more usual. There were no episodes of ventricular fibrillation. In two preparations, delivery of a stimulus closely coupled to the previous spontaneous ventricular depolarization could reliably terminate the arrhythmia. These features, notably the ability to initiate and terminate ventricular tachycardia with single stimuli, indicate the presence of an excitable gap (an interval in the tachycardia cycle in which tissue is able to respond to a stimulus) (50) and support a reentrant mechanism (43). The model therefore provides evidence for the hypothesis that reduced tissue *excitability* of itself can promote tachycardias as a result of functional conduction block (51), presumably leading to spiral wave break-up and thereby to reentrant excitation (47, 49, 50).

Summary/Conclusions

We have thus shown that disruption of the cardiac sodium channel in homozygous *Scn5a*$^{-/-}$ mice leads to a severe defect in ventricular morphogenesis. Heterozygous disruption decreases total sodium conductance, leading directly to impaired action potential propagation, conduction block, and reentrant arrhythmias. These defects in impulse initiation and conduction (23) provide a background for understanding the pathophysiology of several pleiotropic clinical phenotypes (3, 4, 16, 17, 19, 20). Accordingly, the basis for isolated cardiac conduction disease (17), progressive cardiac conduction disorder (16), and the arrhythmogenic substrate in idiopathic ventricular fibrillation (19) can be viewed as involving slowed myocardial conduction (52). These results taken together with those obtained from computer modeling (17, 38) and clinical observations (3, 4) suggest that slow conduction as a result of sodium channel dysfunction represents a critical target for understanding (3, 5, 23) and managing cardiac arrhythmias.

We thank Sandra Webb and Wayne Davies for assistance with the morphological analysis of mouse embryos. This work was supported by the British Heart Foundation, the Medical Research Council, the Helen Kirkland Fund for Cardiac Research, and the Leverhulme Trust. P.M.R.W. holds a Medical Research Council Studentship, C.E.G.H. holds a Medical Research Council Clinical Training Fellowship, P.A.B. holds a Mayo Foundation Scholarship, and J.I.V. holds a British Heart Foundation Basic Science Lectureship. W.H.C. was supported by a Royal Society Leverhulme Research Fellowship, and A.A.G. is a British Heart Foundation Senior Fellow.

1. Spooner, P. M. & Rosen, M. R., eds. (2001) *Foundations of Cardiac Arrhythmias: Basic and Clinical Approaches* (Dekker, New York).
2. The Sicilian Gambit (2001) *Cardiovasc. Res.* **52,** 345–360.
3. Keating, M. T. & Sanguinetti, M. C. (2001) *Cell* **104,** 569–580.
4. Marban, E. (2002) *Nature (London)* **415,** 213–218.
5. Roden, D. M., Balser, J. R., George, A. L., Jr., & Anderson, M. E. (2002) *Annu. Rev. Physiol.* **64,** 431–475.
6. Wang, Q., Shen, J., Splawski, I., Atkinson, D., Li, Z., Robinson, J. L., Moss, A. J., Towbin, J. A. & Keating, M. T. (1995) *Cell* **80,** 805–811.
7. Grant, A. O. (2001) *Am. J. Med.* **110,** 296–305.
8. Zareba, W., Moss, A. J., Schwartz, P. J., Vincent, G. M., Robinson, J. L., Priori, S. G., Benhorin, J., Locati, E. H., Towbin, J. A., Keating, M. T., *et al.* (1998) *N. Engl. J. Med.* **339,** 960–965.
9. Bennett, P. B., Yazawa, K., Makita, N. & George, A. L., Jr. (1995) *Nature (London)* **376,** 683–685.
10. Chandra, R., Starmer, C. F. & Grant, A. O. (1998) *Am. J. Physiol.* **274,** H1643–H1654.
11. Clancy, C. E. & Rudy, Y. (1999) *Nature (London)* **400,** 566–569.
12. Wehrens, X. H., Abriel, H., Cabo, C., Benhorin, J. & Kass, R. S. (2000) *Circulation* **102,** 584–590.
13. Nuyens, D., Stengl, M., Dugarmaa, S., Rossenbacker, T., Compernolle, V., Rudy, Y., Smits, J. F., Flameng, W., Clancy, C. E., Moons, L., *et al.* (2001) *Nat. Med.* **7,** 1021–1027.
14. Gellens, M. E., George, A. L., Jr., Chen, L. Q., Chahine, M., Horn, R., Barchi, R. L. & Kallen, R. G. (1992) *Proc. Natl. Acad. Sci. USA* **89,** 554–558.
15. Wang, Q., Li, Z., Shen, J. & Keating, M. T. (1996) *Genomics* **34,** 9–16.
16. Schott, J. J., Alshinawi, C., Kyndt, F., Probst, V., Hoorntje, T. M., Hulsbeek, M., Wilde, A. A., Escande, D., Mannens, M. M. & Le Marec, H. (1999) *Nat. Genet.* **23,** 20–21.
17. Tan, H. L., Bink-Boelkens, M. T., Bezzina, C. R., Viswanathan, P. C., Beaufort-Krol, G. C., van Tintelen, P. J., van den Berg, M. P., Wilde, A. A. & Balser, J. R. (2001) *Nature (London)* **409,** 1043–1047.
18. Kyndt, F., Probst, V., Potet, F., Demolombe, S., Chevallier, J. C., Baro, I., Moisan, J. P., Boisseau, P., Schott, J. J., Escande, D. & Le Marec, H. (2001) *Circulation* **104,** 3081–3086.
19. Chen, Q., Kirsch, G. E., Zhang, D., Brugada, R., Brugada, J., Brugada, P., Potenza, D., Moya, A., Borggrefe, M., Breithardt, G., *et al.* (1998) *Nature (London)* **392,** 293–296.
20. Alings, M. & Wilde, A. (1999) *Circulation* **99,** 666–673.
21. Balser, J. R. (1999) *Circ. Res.* **85,** 872–874.
22. Vatta, M., Dumaine, R., Varghese, G., Richard, T. A., Shimizu, W., Aihara, N., Nademanee, K., Brugada, R., Brugada, J., Veerakul, G., *et al.* (2002) *Hum Mol. Genet.* **11,** 337–345.
23. Cranefield, P. F. (1975) *The Conduction of the Cardiac Impulse: The Slow Response and Cardiac Arrhythmias* (Futura, Mount Kisco, NY).
24. Noble, D. (1979) *The Initiation of the Heartbeat* (Clarendon, Oxford), pp. 43–52.
25. Marban, E., Yamagishi, T. & Tomaselli, G. F. (1998) *J. Physiol.* **508,** 647–657.
26. Zernicka-Goetz, M., Pines, J., McLean Hunter, S., Dixon, J. P., Siemering, K. R., Haseloff, J. & Evans, M. J. (1997) *Development (Cambridge, U.K.)* **124,** 1133–1137.
27. Zhang, Y., Buchholz, F., Muyrers, J. P. & Stewart, A. F. (1998) *Nat. Genet.* **20,** 123–128.
28. Knopp, A., Thierfelder, S., Koopmann, R., Biskup, C., Bohle, T. & Benndorf, K. (1999) *Cardiovasc. Res.* **41,** 629–640.
29. Benndorf, K. (1994) *J. Gen. Physiol.* **104,** 801–820.
30. Eloff, B. C., Lerner, D. L., Yamada, K. A., Schuessler, R. B., Saffitz, J. E. & Rosenbaum, D. S. (2001) *Cardiovasc. Res.* **51,** 681–690.
31. Bethell, H. W., Vandenberg, J. I., Smith, G. A. & Grace, A. A. (1998) *Am. J. Physiol.* **275,** H551–H561.
32. Saumarez, R. C. & Grace, A. A. (2000) *Cardiovasc. Res.* **47,** 11–23.
33. Rottbauer, W., Baker, K., Wo, Z. G., Mohideen, M. A., Cantiello, H. F. & Fishman, M. C. (2001) *Dev. Cell* **1,** 265–275.
34. Baruscotti, M., DiFrancesco, D. & Robinson, R. B. (2000) *Am. J. Physiol.* **279,** H2303–H2309.
35. VanderBrink, B. A., Sellitto, C., Saba, S., Link, M. S., Zhu, W., Homoud, M. K., Estes, N. A., 3rd, Paul, D. L. & Wang, P. J. (2000) *J. Cardiovasc. Electrophysiol.* **11,** 1270–1276.
36. Meijler, F. L. & Janse, M. J. (1988) *Physiol. Rev.* **68,** 608–647.
37. Petrecca, K., Amellal, F., Laird, D. W., Cohen, S. A. & Shrier, A. (1997) *J. Physiol.* **501,** 263–274.
38. Shaw, R. M. & Rudy, Y. (1997) *Circ. Res.* **81,** 727–741.
39. Wickman, K., Nemec, J., Gendler, S. J. & Clapham, D. E. (1998) *Neuron* **20,** 103–114.
40. Platzer, J., Engel, J., Schrott-Fischer, A., Stephan, K., Bova, S., Chen, H., Zheng, H. & Striessnig, J. (2000) *Cell* **102,** 89–97.
41. Kass, D. A., Hare, J. M. & Georgakopoulos, D. (1998) *Circ. Res.* **82,** 519–522.
42. Saumarez, R. C., Heald, S., Gill, J., Slade, A. K., de Belder, M., Walczak, F., Rowland, E., Ward, D. E. & Camm, A. J. (1995) *Circulation* **92,** 2565–2571.
43. Antzelevitch, C. (2001) *Curr. Opin. Cardiol.* **16,** 1–7.
44. Sakmann, B. F., Spindler, A. J., Bryant, S. M., Linz, K. W. & Noble, D. (2000) *Circ. Res.* **87,** 910–914.
45. Ashamalla, S. M., Navarro, D. & Ward, C. A. (2001) *J. Physiol.* **536,** 439–443.
46. Zygmunt, A. C., Eddlestone, G. T., Thomas, G. P., Nesterenko, V. V. & Antzelevitch, C. (2001) *Am. J. Physiol.* **281,** H689–H697.
47. Janse, M. J. & Downar, E. (2001) in *Foundations of Cardiac Arrhythmias: Basic and Clinical Approaches*, eds. Spooner, P. M. & Rosen, M. R. (Dekker, New York), pp. 449–477.
48. Roden, D. M. (2001) in *Foundations of Cardiac Arrhythmias: Basic and Clinical Approaches*, eds. Spooner, P. M. & Rosen, M. R. (Dekker, New York), pp. 21–41.
49. Vaidya, D., Morley, G. E., Samie, F. H. & Jalife, J. (1999) *Circ. Res.* **85,** 174–181.
50. Cabo, C., Pertsov, A. M., Davidenko, J. M., Baxter, W. T., Gray, R. A. & Jalife, J. (1996) *Biophys. J.* **70,** 1105–1111.
51. Rohr, S., Kucera, J. P. & Kleber, A. G. (1998) *Circ. Res.* **83,** 781–794.
52. Gussak, I., Bjerregaard, P. & Hammill, S. C. (2001) *J. Am. Coll. Cardiol.* **37,** 1635–1638.